Origin of Individuality of Two Daughter Cells during the Division Process Examined by the Simultaneous Measurement of Growth and Swimming Property Using an On-Chip Single-Cell Cultivation System

Senkei Umehara, Ippei Inoue, Yuichi Wakamoto, and Kenji Yasuda
Department of Biomedical Information, Division of Biosystems, Institute of Biomaterials and Bioengineering, Tokyo Medical and Dental University, 2-3-10 Kanda-Surugadai, Chiyoda-ku, Tokyo 101-0062, Japan

ABSTRACT We examined the origin of individuality of two daughter cells born from an isolated single *Escherichia coli* mother cell during its cell division process by monitoring the change in its swimming behavior and tumbling frequency using an on-chip single-cell cultivation system. By keeping the isolated condition of an observed single cell, we compared its growth and swimming property within a generation and over up to seven generations. It revealed that running speed decreased as cell length smoothly increased within each generation, whereas tumbling frequency fluctuated among generations. Also found was an extraordinary tumbling mode characterized by the prolonged duration of pausing in predivisional cells after cell constriction. The observed prolonged pausing may imply the coexistence of two distinct control systems in a predivisional cell, indicating that individuality of daughter cells emerges after a mother cell initiates constriction and before it gets physically separated into two new cell bodies.

INTRODUCTION

Cells gather information both from their ancestors and from their surroundings. Some information affects the cells temporarily; some affects them over successive generations. Whether information is inheritable or not should therefore be important when the quality of information is discussed.

In the context of information inheritance, there arises a question about the definition of a ''generation'' of cells. A conventional generation spans the period between birth and division of an individual. In the case of the Gram-negative bacteria *Escherichia coli*, which are single-celled organisms, a generation starts when a cell is born as a portion (usually a half) of its mother cell and ends when that cell itself divides into its daughter cells. Nobody knows, however, whether or not the information in *E. coli* is inherited at exactly the time of cell division. One could think that a mother cell finished bequeathing genetic information and separated the cellular components carrying information about cellular functions into two parts while preparing for the coming cell division.

A direct approach to the question is to continuously observe a particular cellular function, such as chemotactic cellular motility, as an index of cellular information as the cell grows. The overall movement of a bacterium is caused by movement modes alternating between ''running'' (swimming smoothly in one direction) and ''tumbling'' (randomly changing swimming direction); and an *E. coli* cell responding to an attractant or repellent chemical directs its overall movement along the chemical gradient by making apparently purposeful changes in its modes of movement (1). This response is regulated by a complicated signal transduction network. Overall swimming behavior has been investigated by measuring swimming speed and flagellar rotation rate (2) as well as tumbling frequency (3); and the relations between growth, motility, swimming speed, and growth phases have also been investigated (4). The flagellar master operon *flhD* has been found to affect cell division (5) and might control the synthesis of individual flagella over several generations (6).

Detecting changes in the swimming behavior of a particular line of growing cells seems feasible but has been challenging many scientists because it is experimentally difficult. It is impossible to follow direct descendant cells in a test tube, and even if they were identified they could not be observed continuously as they grow. Clearly identifying transient time-course changes in a particular function is difficult, and they must be investigated separately because they might provide information about the relation between growth and motility but not about when the individuality of a particular cell arises.

We have overcome these experimental limitations by developing a system that measures growth and motility simultaneously (7,8). Its single-cell-based dual-recording feature has made it possible to directly compare the cellular growth and motility of a cell with that of its direct descendants. The results it can provide will not only help answer the question about the definition of a generation but will also give us the information we need to reinterpret and integrate previous studies.

Submitted September 25, 2006, and accepted for publication April 5, 2007.

Address reprint requests to Kenji Yasuda, PhD, Dept. of Biomedical Information, Division of Biosystems, Institute of Biomaterials and Bioengineering, Tokyo Medical and Dental University, 2-3-10 Kanda-Surugadai, Chiyoda-ku, Tokyo 101-0062, Japan. Tel.: 81-3-5280-8046; Fax: 81-3-5280-8049; E-mail: yasuda.bmi@tmd.ac.jp.

Editor: Elliot L. Elson.

0006-3495/07/08/1061/07 $2.00

doi: 10.1529/biophysj.106.098061

MATERIALS AND METHODS

On-chip single-cell microcultivation system

An on-chip single-cell microcultivation system is needed if we are to follow the activities of a particular single swimming cell for many generations (9–11). This system used in the work reported here (shown in Fig. 1) contains a microchamber array plate, optical tweezers, a buffer exchange unit, and a microscope with a 60× phase-contrast object lens.

The microchamber array plate is a 0.1-mm-thick cover glass on which were fabricated 12 × 12 arrays of micrometer-size structures called microchambers, where cells were cultivated. They were made of SU-8, a thick negative photoresist (Microlithography Chemical, Newton, MA), and each microchamber was 115 μm × 80 μm × 4 μm. After the sample cells are put into the array, it was covered with a semipermeable membrane (molecular weight cutoff = 25,000; Spectrum Laboratories) coated with streptavidin. It attached so tightly to the glass substrate, which had been coated with biotin beforehand, that it prevented the cells in the microchambers from escaping.

Optical tweezers were used as a noncontact handling tool when unwanted cells needed to be removed (Fig. 2). We sent the light from a neodymium-doped yttrium aluminum garnet laser (wavelength = 1064 nm; T20-8S, Spectra-Physics, Mountain View, CA) through a 60× phase-contrast oil-immersion object lens (PlanApo, numerical aperture = 1.4, Olympus, Tokyo, Japan). This laser enabled us to manipulate a cell in the field of view. Immediately after cell divisions, we used it to remove one of the two newborn cells into a trapping region within a microchamber.

A buffer exchange unit consists of a medium tank, thin plastic tubes, a peristaltic pump, a waste tank, and a 1-mL glass cube called a cover chamber. This cover chamber, a cube with two branches on opposite side surfaces and with one of the orthogonal sides open, was mounted with the open side against the microchamber array plate and was sealed to that plate. Fresh medium pumped from the medium tank at ~10 mL/h passed through the cover chamber and reached the waste tank. This continuous flow maintained a uniform condition around the cultured cells in a microchamber covered with semipermeable membrane.

Phase-contrast microscopy (with a 60× objective) was set up with an Olympus IX-71. Images were acquired with a charge-coupled device camera (CS230, Olympus) and recorded on a digital videocassette recording (VCR) system.

Bacterial strain and growth conditions

A plasmid coding a fusion protein of aspartate receptor and green fluorescent protein (Tar-GFP) was introduced to *E. coli* strain AW539 (AW405 *tar*$^-$) (12), obtained from Dr. Ikuro Kawagishi of Nagoya University. The growth and motility of this resultant strain, AW539/pTar-GFP, were indistinguishable from those of the wild-type (data not shown).

Sample preparation started with the reactivation of the frozen cell stock. They were reactivated by culturing them, without shaking, overnight in Luria-Bertani (LB) medium at room temperature. Sample motile cells at their mid- to late-log phase were then obtained by diluting a portion of the reactivated stationary-phase culture in 1 mL of LB medium and cultivating it under the same conditions for 3 h. After the sample cells were sealed in microchambers covered with a semipermeable membrane, the sample slide on which the cover chamber was mounted was set on a microscope stage. One microchamber was chosen for continuous single-cell observation, during which fresh LB medium at room temperature was continuously circulated.

Repeated isolation was performed every time the observed cell divided into two daughter cells. The newborn daughter cell that was discarded in this step was the one that was longer or showed less motility. If the two daughter cells were indistinguishable, the one discarded was chosen randomly.

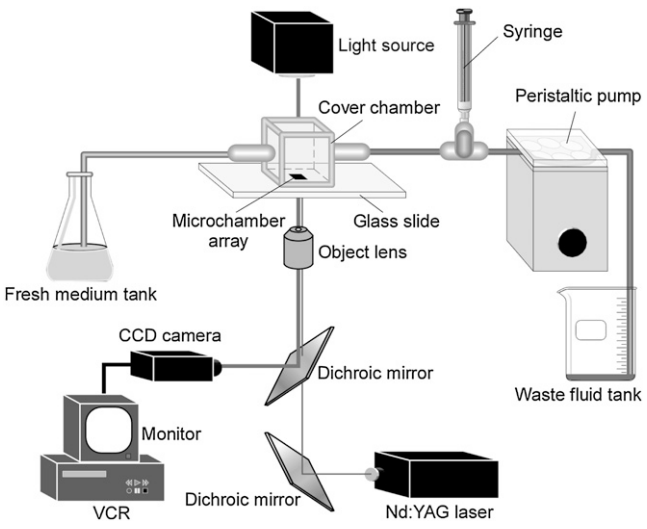

FIGURE 1 Design of the on-chip single-cell cultivation system.

Measuring procedure

We designed analysis software based on LabVIEW (National Instruments, Austin, TX). It measured parameters describing the growth and swimming behavior of the cell, both in real time and in recorded microscope images. Directly measured parameters were cell position, cell size, and the direction of cell motion. This program ran for hours and acquired the parameters with 0.1-s resolution.

Cell length, running speed, and tumbling frequency were determined from the measured parameters. Cell length was determined by extracting the maximum value within each 5-min period to avoid underestimating the length from images in which the cell looks either defocused or three-dimensionally oriented against the planar surface.

Running speed, v, was calculated from selected data sets confirmed to be those of cells in pure run-mode motion (without tumble-mode motion). It was calculated as

$$v = \frac{1}{N} \sum_{t_i < t_1, t_2 < t_f} \frac{|\vec{r}_1 - \vec{r}_2|}{|t_1 - t_2|} \quad (|t_1 - t_2| \le 0.5),$$

where t_i and t_f (s) are the starting and ending times of the 5-min calculation periods, t_1 and t_2 (s) are the given time points included in the periods, r_1 and r_2 (μm) are the positions of the cell at t_1 and t_2, and N is the total number of time points included in the periods. In other words, running speed, v (μm/s), is the mean value of ''instantaneous'' speed measured with 0.1-s resolution.

Tumbling frequency was calculated from the number of times that tumbling behavior was counted by eye in real time. We defined tumbling as a sudden stop in motion, regardless of the direction in which the cell moved after stopping. The number of tumblings and the duration of each tumbling were saved in a computer file, and all such files were later integrated into one file to be processed. Calculation was based on two replicates to reduce counting errors.

RESULTS

Repeated isolation of swimming cells

Repeated isolation of the observed cell was essential not only to identify it but also to strictly control the surrounding conditions (the chance of physical contact with other cells, possible secretions from them, and other environmental factors). As in our previously reported work dealing with nonmotile cells (9–11), we removed unwanted motile cells one by one with optical tweezers. The descendent cells of a particular single cell could be cultivated for successive generations,

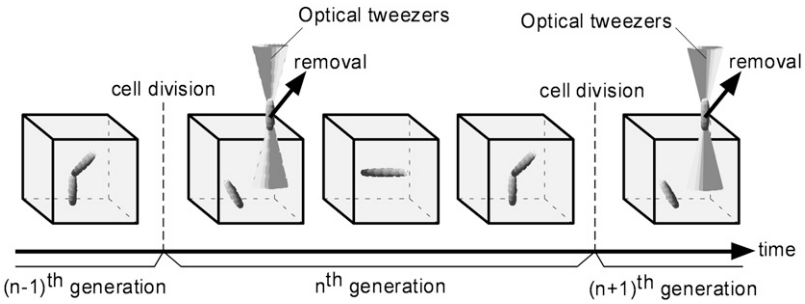

FIGURE 2 Schematic diagram of the single-cell cultivation method. Long-term single-cell observation was achieved by keeping observed cells isolated. Immediately after the cell division, we removed one of the two newborn daughter cells with optical tweezers. Abnormal cells in terms of cell length or swimming behavior were preferably chosen to be removed; otherwise the removed cell was chosen at random. This procedure allowed the other daughter cell to remain isolated as the next generation cell. Every time the observed cell divided we went through the same routine.

whereas leaving the cell as it proliferated resulted in a dense mixture of its descendant cells (Fig. 3). Trapped cells exposed to the focused laser for a few minutes no longer elongated or swam.

Simultaneous measurement of growth and motility

A typical result of simultaneous measurement of cell length and running speed is summarized in Fig. 4. Fig. 4 *a* is a record of cell length and running speed for one generation, from the birth of a cell to that of its daughter cells. Throughout its cell cycle the cell steadily elongated exponentially. Its running speed, on the other hand, gradually decreased throughout the cycle. The running speed was calculated on the basis of the recorded positions of the cell. By plotting these positions, we can also generate the swimming path of the cell for an arbitrarily defined time range (Fig. 4 *b*). Each position was determined by an image analysis program driven in real time with 0.1-s resolution. The program recognized the positions of the cell based on a successive series of high-resolution images (Fig. 4 *c*).

Comparison between successive generations

By combining the repeated isolation procedure with this analysis, we can compare the growth and motility of an isolated single cell with the growth and motility of its direct descendants. Fig. 5 is an example of simultaneous measurements for seven generations. The cell length smoothly increased within each cell cycle (Fig. 5 *a*). The running speed decreased throughout each cell cycle (Fig. 5 *b*). Within each cell cycle the plots of running speed versus generation time tended to form smooth curves, but the slopes of those curves differed between one generation and another. Tumbling frequency fluctuated between generations and did not show any constant increase or decrease (Fig. 5 *c*). Both the decrease in speed and the fluctuation in tumbling frequency were reproducible among other data sets (Table 1).

Prolonged pausing found in the final stage of cell cycles

Careful observation revealed that a predivisional cell after constriction showed characteristic movement (movies available as Supplementary Material). It can be characterized by a

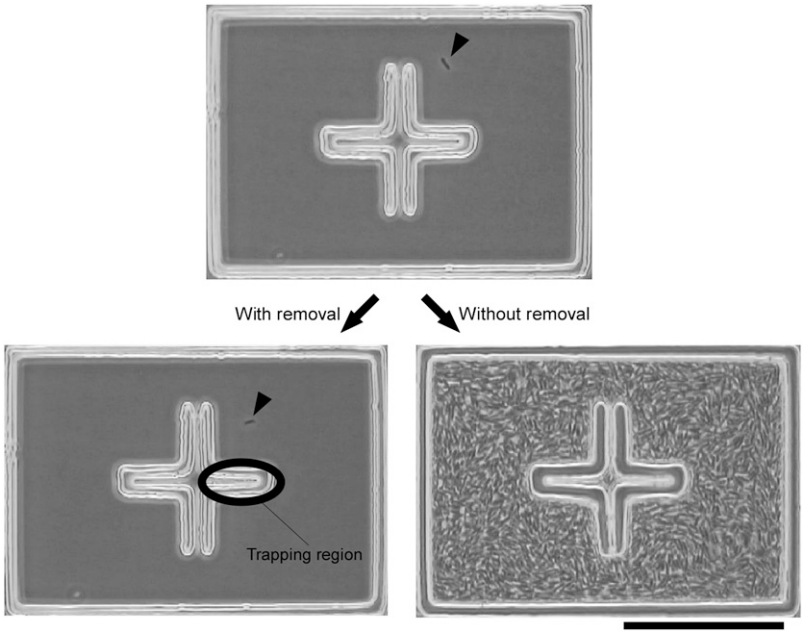

FIGURE 3 The effect of cell isolation with optical tweezers. Repeated removal of unwanted cells was necessary to achieve the long-term observation of a single *E. coli* cell. Continuous optical trapping in the trapping region inhibited both growth and motility of freely swimming cells, allowing the observed cell (*arrowhead*) to swim around in the isolated condition for up to 11 generations (*left*). Without this isolation process, the microchamber was filled with proliferated descendant cells (*right*). Bar, 50 μm.

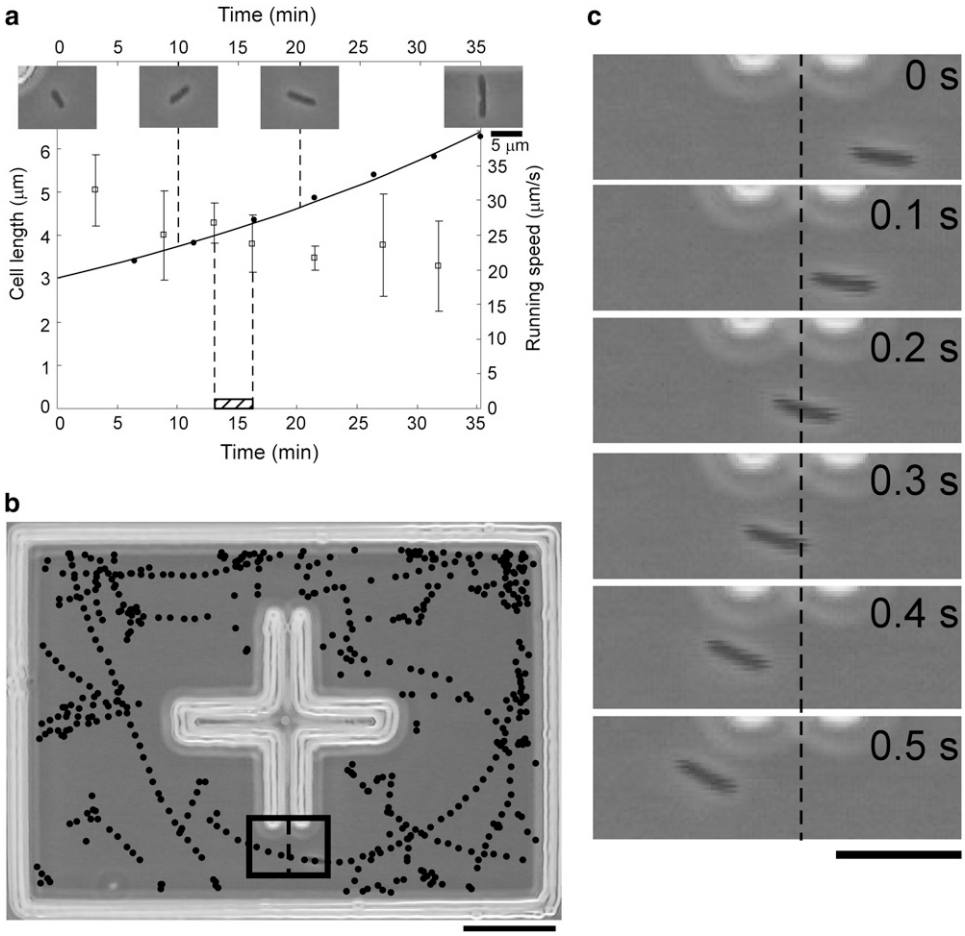

FIGURE 4 Typical example of simultaneous measurement of growth and motility. (*a*) Time course of single *E. coli* growth and motility for one cell cycle (t = 0–35.3). Cell length (*solid circles* with a fitted exponential growth curve) steadily increased as the running speed (*open squares* with standard deviation) decreased throughout the cell cycle. Photographs show the morphology of the cell at each corresponding time point. (*b*) Swimming path of the cell. Black dots are recognized positions of the cell by the computer analysis program for the hatched time range shown in (*a*) (t = 13.0–16.2). Bar, 20 μm. (*c*) Photographs of the signified region in (*b*) at successive 0.1-s frames. The cell was swimming through the region from right to left. Bar, 10 μm.

longer duration of pausing in motion: typically 10^{-1}–10^{0} s, which is about 10 times longer than that caused by ordinary tumbling (10^{-2}–10^{-1} s). We named it ''prolonged pausing'' in contrast to ordinary tumbling. To analyze it in a quantitative manner, we measured the duration of each pausing in motion and averaged it in a 1-min time window (Fig. 6). The duration of pausing remained relatively constant before cell constriction, but it tended to increase after constriction to the level beyond the deviation from the preconstriction value (generation 5 seemed to be an exception). The increase in pausing duration appeared only after cell constriction, reflecting that only predivisional cells exhibit prolonged pausing.

DISCUSSION

Validity and significance of simultaneous single-cell measurement

The results of this on-chip measurement were consistent with the results of conventional methods. The measured running speed and tumbling frequency were both acceptable when compared to those that have already been reported for the wild-type strain (25 μm/s (1) and 0.53 s^{-1} (13)). This means that the microchambers confining the cells did not affect the swimming behavior and that the on-chip measurement was compatible with other conventional methods.

More important is that we have measured growth and motility separately but simultaneously. Conventional methods cannot deal with both of them because growth needs to be watched for a longer term, whereas motility requires close observation for a shorter term. Moreover, conventionally obtained results describe only the average characteristics of a group of cells. The improved on-chip single-cell cultivation system that copes with swimming bacteria has overcome these limitations. We have shown a direct relation between growth and motility: cell-cycle dependence of swimming behavior.

Similarity in the speed curves

The smooth speed curves imply that the running speed of a cell is determined by the physical properties of that cell rather than by its active control during the cell cycle. This idea was also supported by the calculation of the torque generated by cells. Because of the low Reynolds number of the motion of microbes through liquids ($\sim 3 \times 10^{-5}$ (14)), torque generated by a cell is proportional to the drag force

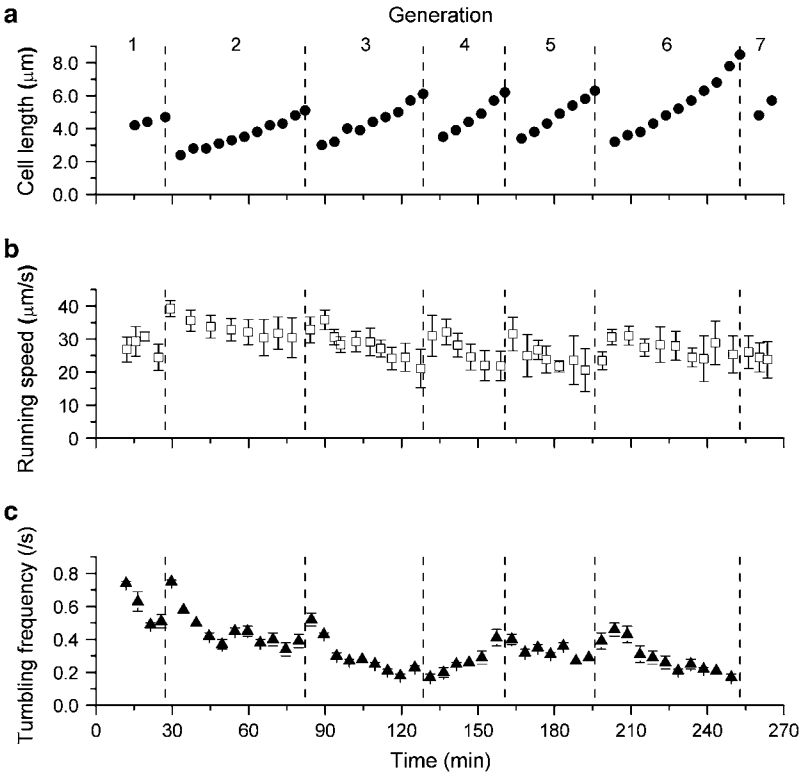

FIGURE 5 Simultaneous measurement of growth and motility for successive generations. Time course of single *E. coli* growth and motility were monitored by the measurement of (*a*) cell length, (*b*) running speed (mean ± SD), and (*c*) tumbling frequency (mean ± SE). Vertical dashed lines correspond to the timing of cell divisions.

exerted by the fluid. Table 2 summarizes the calculation results for the cells of generations 2–6 in Fig. 5 (see Appendix for details about the calculation). Except for generation 6, when the cell was extraordinarily elongated, little difference was seen between the torque generated in the initial and final stages of cell cycles. If the cell controlled its own motility, change in torque generation should have appeared.

The constancy of torque generation may be explained by the saturation of motor rotation. Unlike tethered cells, freely swimming cells are under a low-load condition in which flagella are reported to run far from saturated condition (15). If the motors operate at maximal speed, running speed should be governed by the physical properties of the cell.

TABLE 1 Statistics on running speed and tumbling frequency within a generation

	Running speed		Tumbling frequency	
	Mean ± SD (μm/s)	Final/initial*	Mean ± SD (s^{-1})	Final/initial
Initial half of the cell cycle	25.3 ± 7.0	0.83 ± 0.14	0.68 ± 0.50	0.95 ± 0.43
Final half of the cell cycle	21.2 ± 7.1		0.58 ± 0.36	
n	23		16	

*The ratio ''final/initial'' was calculated with a pair of the values for each generation, and the mean ± SD of all the generations is shown in the table. Note that the calculation result, for instance $0.95 = \Sigma(f_{final}/f_{initial})/n$ in the case of mean tumbling frequency, is not equal to the ratio of the average of f_{final}, $0.58 = \Sigma f_{final}/n$, to that of $f_{initial}$, $0.68 = \Sigma f_{initial}/n$.

Fluctuation in tumbling frequency

Unlike the running speed of a cell that may be determined by its physical properties, the switching behavior between running and tumbling is known to reflect intracellular conditions. By analyzing intergenerational relationships, we might be able to discuss if any information, especially epigenetic information that affects the switching behavior, is transmitted to next generations. Currently our results indicate that the tumbling frequency of a mother cell fluctuates and does not necessarily correlate with that of its daughter cells, which means that the information in a mother cell could be lost at or before cell division. In this case, little or no information about the switching is inherited from a mother cell, and a daughter cell therefore behaves as an independent entity. To further elucidate the issue on the possible heritable information, correlation between a mother and both of its two daughters, as well as that between the two ''twin'' daughters, should be intensively investigated.

Emergence of individuality in predivisional mother cells

We found prolonged pausing that appeared exclusively in the final stage of cell cycles, after the initiation of cell constriction. This prolonged pausing in predivisional cells poses an important question about the emergence of individuality of the subsequent daughter cells.

Mother cells and daughter cells are usually defined by cell division: a physical process that divides the cell body into

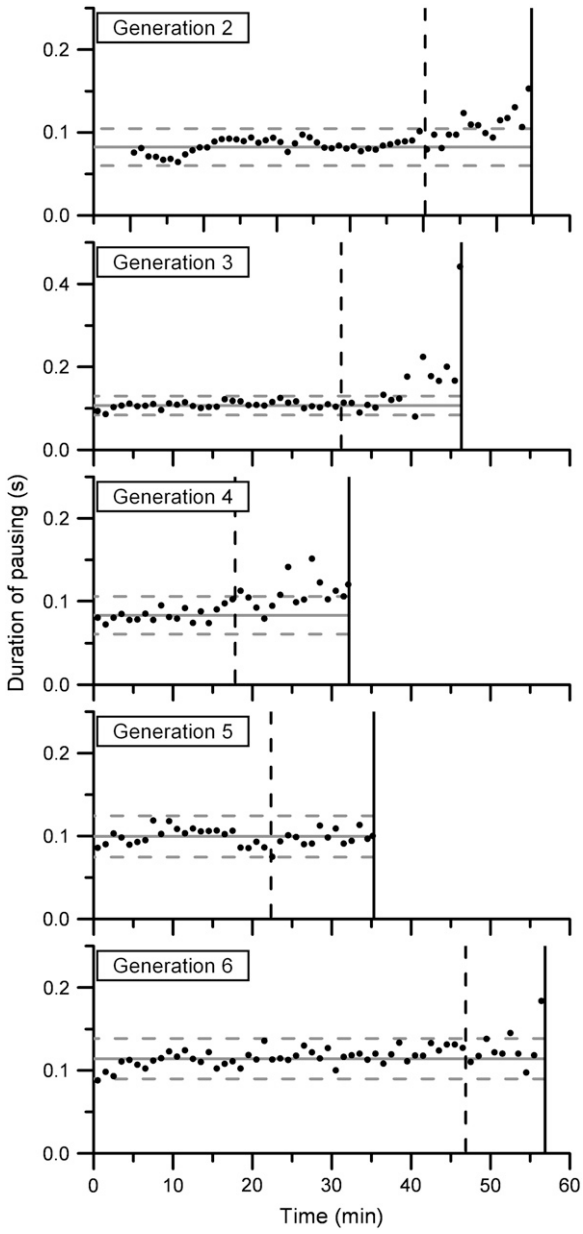

FIGURE 6 Prolonged pausing found in the final stage of cell cycles. Duration of pausing per each tumbling was averaged in a time window of 1 min and plotted as a function of time for generations 2–6 (same as Fig. 5) with the timing of cell division (*vertical solid lines*) as well as the initiation of cell constriction (*vertical dashed lines*). Compared to the mean values before constriction (*horizontal solid lines*, mean; *horizontal dashed lines*, standard deviation), the duration tended to increase in the final stage of cell cycles.

two newborn ones. To complete cell division and to become two cells, however, a cell must spend some time preparing at molecular and cellular levels. Thus there must be a transient state in which two distinct control systems coexist in a predivisional cell. These two systems would independently affect the intracellular mechanism for the whole-cell moving behavior.

TABLE 2 Calculated torque generated by direct descendant cells regarded as spheroids

Generation		Length (μm)	Width (μm)	K*	Speed (μm/s)	Drag force (pN)	Torque ratio: final/initial
2	Initial	2.3	1.0	1.26	39.2	0.42	1.0
	Final	4.7	1.0	1.70	30.4	0.44	
3	Initial	2.8	1.0	1.35	32.8	0.38	0.9
	Final	6.0	1.0	1.92	21.0	0.35	
4	Initial	3.2	1.0	1.42	30.9	0.38	1.0
	Final	5.9	1.0	1.92	21.8	0.36	
5	Initial	3.2	1.0	1.43	31.5	0.39	0.9
	Final	5.9	1.0	1.91	20.5	0.34	
6	Initial	2.9	1.0	1.36	23.4	0.28	1.8
	Final	7.9	1.0	2.22	25.3	0.49	

*The correction to Stokes' law. See Appendix for details.

Prolonged pausing, which appeared between the initiation of cell constriction and the physical separation into two new cell bodies, is probably reflecting this behavior. After the initiation of cell constriction, cellular contents are segregated into two daughters-to-be by an internal structure called a septum. During the segregation process it is likely that switching in one daughter-to-be cannot be synchronized smoothly with that in the other daughter-to-be. This asynchronous state may have been observed as prolonged pausing. Because of its characteristic movement it differs from pausing of antibiotic-treated filamentous cells, shown to be equivalent to ordinary tumbling of normal-sized cells (16). Rather we hypothesize that the observed prolonged pausing reflects the coexistence of two distinct control systems within a mother cell; that is, individuality emerges after a single cell initiates constriction and before it gets physically separated into two new cell bodies.

Individuality has also been discussed from the viewpoint of bacterial swimming behavior by Spudich and Koshland (3). They reported that cellular individuality in bacteria is rather steady throughout their cell cycles. Although the phenomenon in this report looks like the opposite from our results, it does not contradict this study because they regarded cell length as an index of cell cycles and they neglected the fluctuation of synchrony between cell length and cell cycle. Since even direct descendant cells vary in length (11), we cannot infer that different cells of the same cell length are at the same stage of their cell cycles. The prolonged pausing we have found here was probably hidden by this large variation and was revealed by the long-term single-cell monitoring.

Prolonged pausing requires further investigation. We have tried to visualize the corresponding flagella movement but failed because of the difficulty of visualizing it in growing cells. Dark field microscopy was not appropriate for long-term observation because the light to which cells were exposed impaired their motility. Although fluorescence did permit long-term observation, it impaired cellular growth. Because prolonged pausing usually appears only just before

cell division, cells displaying prolonged pausing were too rare to find. And should they be found, it would be impossible to prove that they are actually in the final stage of their cell cycles.

In summary, this work introduced an application of an on-chip single-cell cultivation system that allows the simultaneous measurement of growth and swimming property for successive generations. By monitoring cell length, running speed, and tumbling frequency of isolated single *E. coli* cells, we found the decrease in running speed within a generation, fluctuation in tumbling frequency over generations, and prolonged pausing that only appears in the final stage of cell cycles. We hypothesized that the observed prolonged pausing is related to the coexistence of two distinct control systems within a single cell, indicating that individuality of daughter cells arises between the initiation of cell constriction and the physical separation of the cell body.

APPENDIX: CALCULATION OF TORQUE GENERATED BY A CELL

The driving force for a cell swimming at a constant speed in a viscous medium is equal to the resistance that produces drag force, and at low speeds the dominant resistance is that due to viscosity. According to Happel and Brenner's low Reynolds number hydrodynamics (17), the drag force on a prolate spheroid in a uniform flow is therefore given by a corrected form of Stokes' law: $F = -6\pi\mu bUK$ where μ is the coefficient of viscosity; b the equatorial radius; U the flow velocity; and K the correction factor due to the differing polar and equatorial radii. Here K is a geometric parameter determined solely by the ratio of the longer axis to the shorter axis of the spheroid. For prolate spheroids, K is calculated to be <1 (see Table 4 26.1 in Happel and Brenner (17) for the calculation results), resulting in the increase in resistance. The F values were calculated by substituting the viscosity of water at 25°C (8.90×10^{-4} Pa/s) for μ, half of the cell width for b, running speed for U, and calculated K based on the measured cell length/cell width ratio.

SUPPLEMENTARY MATERIAL

To view all of the supplemental files associated with this article, visit www.biophysj.org.

An *Escherichia coli* strain AW539 (AW405 *tar*$^-$) (12) was kindly provided by Drs. Ikuro Kawagishi and Daisuke Shiomi.

Financial support by Grants-in-Aid for Scientific Research and a Grant-in-Aid for JSPS Fellows from the Ministry of Education, Culture, Sports, Science and Technology of Japan and the Japan Science and Technology Agency is gratefully acknowledged.

REFERENCES

1. Stock, J. B., and M. G. Surette. 1996. Chemotaxis. *In Escherichia coli* and *Salmonella*: Cellular and Molecular Biology, 2nd ed. F. C. Neidhardt, R. Curtiss III, J. L. Ingraham, E. C. C. Lin, K. B. Low, B. Magasanik, W. S. Rfznikopp, M. Riley, M. Schaechter, and H. E. Umbarger, editors. ASM Press, Washington, DC. 1103–1129.
2. Magariyama, Y., S. Sugiyama, K. Muramoto, I. Kawagishi, Y. Imae, and S. Kudo. 1995. Simultaneous measurement of bacterial flagellar rotation rate and swimming speed. *Biophys. J.* 69:2154–2162.
3. Spudich, J. L., and D. E. Koshland Jr. 1976. Non-genetic individuality: chance in the single cell. *Nature.* 262:467–471.
4. Amsler, C. D., M. Cho, and P. Matsumura. 1993. Multiple factors underlying the maximum motility of *Escherichia coli* as cultures enter post-exponential growth. *J. Bacteriol.* 175:6238–6244.
5. Pruss, B. M., and P. Matsumura. 1996. A regulator of the flagellar regulon of *Escherichia coli*, *flhD*, also affects cell division. *J. Bacteriol.* 178:668–674.
6. Aizawa, S. I., and T. Kubori. 1998. Bacterial flagellation and cell division. *Genes Cells.* 3:625–634.
7. Hattori, A., S. Umehara, Y. Wakamoto, and K. Yasuda. 2003. Measurement of incident angle dependence of swimming bacterium reflection using on-chip single-cell cultivation assay. *Jpn. J. Appl. Phys.* 42: L873–L875.
8. Umehara, S., A. Hattori, Y. Wakamoto, and K. Yasuda. 2004. Simultaneous measurement of growth and movement of cells exploiting on-chip single-cell cultivation assay. *Jpn. J. Appl. Phys.* 43:1214–1217.
9. Umehara, S., Y. Wakamoto, I. Inoue, and K. Yasuda. 2003. On-chip single-cell microcultivation assay for monitoring environmental effects on isolated cells. *Biochem. Biophys. Res. Commun.* 305:534–540.
10. Wakamoto, Y., I. Inoue, H. Moriguchi, and K. Yasuda. 2001. Analysis of single-cell differences by use of an on-chip microculture system and optical trapping. *Fresenius J. Anal. Chem.* 371:276–281.
11. Wakamoto, Y., S. Umehara, K. Matsumura, I. Inoue, and K. Yasuda. 2003. Development of non-destructive, non-contact single-cell based differential cell assay using on-chip microcultivation and optical tweezers. *Sens. Actuators B Chem.* 96:693–700.
12. Mesibov, R., and J. Adler. 1972. Chemotaxis toward amino acids in *Escherichia coli*. *J. Bacteriol.* 112:315–326.
13. Alon, U., L. Camarena, M. G. Surette, B. Aguera y Arcas, Y. Liu, S. Leibler, and J. B. Stock. 1998. Response regulator output in bacterial chemotaxis. *EMBO J.* 17:4238–4248.
14. Kim, M., J. C. Bird, A. J. Van Parys, K. S. Breuer, and T. R. Powers. 2003. A macroscopic scale model of bacterial flagellar bundling. *Proc. Natl. Acad. Sci. USA.* 100:15481–15485.
15. Gabel, C. V., and H. C. Berg. 2003. The speed of the flagellar rotary motor of *Escherichia coli* varies linearly with protonmotive force. *Proc. Natl. Acad. Sci. USA.* 100:8748–8751.
16. Maki, N., J. E. Gestwicki, E. M. Lake, L. L. Kiessling, and J. Adler. 2000. Motility and chemotaxis of filamentous cells of *Escherichia coli*. *J. Bacteriol.* 182:4337–4342.
17. Happel, J., and H. Brenner. 1983. Low Reynolds Number Hydrodynamics. Kluwer, Boston.